

9<sup>th</sup> U. S. National Combustion Meeting  
Organized by the Central States Section of the Combustion Institute  
May 17-20, 2015  
Cincinnati, Ohio

# Computational Study of Turbulent Premixed Counterflow Flames

*Ranjith Tirunagari<sup>1,\*</sup>, Stephen B. Pope<sup>1</sup>*

<sup>1</sup>*Sibley School of Mechanical and Aerospace Engineering, Cornell University, Ithaca, NY,  
14853, USA*

*\*Corresponding Author Email: rrt38@cornell.edu*

**Abstract:** In this paper we report results from a computational study of turbulent premixed counterflow flames. The counterflow burner in this mode consists of two opposed nozzles, one emitting fresh premixed reactants, CH<sub>4</sub>/O<sub>2</sub>/N<sub>2</sub>, the other hot stoichiometric combustion products. This results in a turbulent premixed flame close to the mean stagnation plane. The critical parameters identified in these flames are the bulk strain rate, turbulent Reynolds number, equivalence ratio of the reactant mixture and temperature of the combustion products. A base case simulation involving reference values of these flow parameters is analyzed both in terms of unconditional and conditional statistics. Additionally, the parametric space is explored by studying the effects of three critical parameters - bulk strain rate, turbulent Reynolds number and reactants equivalence ratio - on the turbulent flame behavior. The simulations are carried out using the Large Eddy Simulation/Probability Density Function (LES/PDF) methodology. In this approach, LES is used to represent the flow and turbulence, and the PDF method is used to represent turbulence-chemistry interactions. A new treatment is developed for the inflow velocity boundary conditions at the nozzle exits that can match the mean and r.m.s. velocities and the turbulent length scales in the simulations to those in the experiments. The instantaneous centerline profiles of OH mass fraction are used to identify the interface between the two counterflowing streams referred to as the gas mixing layer interface (GMLI), and the turbulent flame front using a reaction progress variable,  $c$ . The statistics of the mean and r.m.s. velocities and the mean progress variable on the centerline are found to agree well with the experimental data for the base case. More importantly, the probability of localized extinction at the GMLI and the PDF of flame position relative to the GMLI compare well with the experiments for all the flow conditions including the base case.

**Keywords:** *Turbulent premixed flames, LES/PDF, Extinction*

## 1. Introduction

### 1.1 Motivation for a computational study of counterflow flames

In this paper we focus on turbulent counterflow flames (TCF) which provides an alternative configuration to the much more studied jet flames [1]. The TCF configuration has several advantages including (i) the achievement of high Reynolds numbers without pilot flames; (ii) control of the transition from stable flames to local extinction/re-ignition conditions; (iii) compactness of the domain compared with jet flames; (iv) the ability to explore combustion of fuels that include bio-fuels and fuel blends and (v) relevance to practical combustion devices [1]. In particular, we study the turbulent counterflow flame in its premixed mode using the Large-Eddy Simulation/Probability Density Function (LES/PDF) computational methodology. As

## Sub Topic: Turbulent Flames

discussed in more detail in the subsequent sections, the extensive experimental data available for this mode enable us to test our computational models through detailed comparisons.

### 1.2 Yale/Sandia experimental studies

The turbulent premixed counterflow flame is experimentally studied by Coriton et al. [2] in which a systematic study was conducted on the effects of four critical parameters on the interactions of turbulent premixed  $\text{CH}_4/\text{O}_2/\text{N}_2$  flame with stoichiometric counterflowing combustion products. Figure 1 shows the experimental configuration of the premixed mode and its computational counterpart. The base case is described now. The top stream is a highly turbulent stream of a premixed  $\text{CH}_4/\text{O}_2/\text{N}_2$  mixture at a turbulent Reynolds number of  $\text{Re}_t = 1050$  with an equivalence ratio of  $\phi_u = 0.85$  at  $T_u = 294$  K and 1 atm. The turbulence in the top stream is generated by placing a turbulence generating plate (TGP) inside the nozzle. The molar ratio of  $\text{O}_2/\text{N}_2$  is fixed at 30/70 in this stream. The bottom nozzle hosts a pre-burner which burns stoichiometric  $\text{CH}_4/\text{O}_2/\text{N}_2$  mixture to completion, so the bottom stream is a hot stoichiometric combustion products stream with a measured temperature of  $T_b = 1850$  K and 1 atm. Note that the TGP is omitted in the bottom nozzle due to increased viscosity of the burnt combustion products. A turbulent premixed flame is established near the stagnation plane between the two nozzles which are placed at a distance of  $d_{\text{nozzle}} = 16$  mm apart. Based on the bulk velocity of  $U_{\text{bulk}} = 11.2$  m/s in the upper jet, the bulk strain rate  $K_{\text{bulk}}$ , defined as  $K_{\text{bulk}} = 2U_{\text{bulk}}/d_{\text{nozzle}}$ , is  $1400 \text{ s}^{-1}$ .

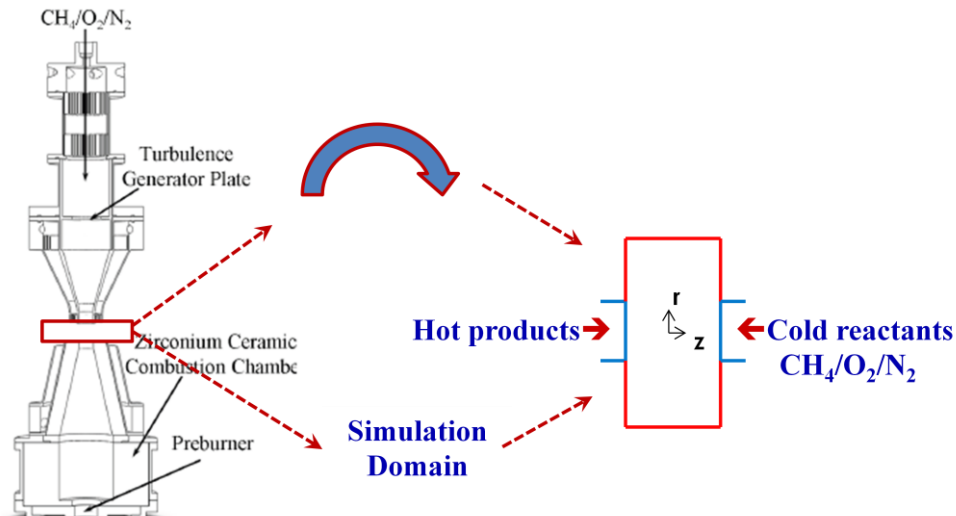


Figure 1: The experimental configuration of the TCF in the premixed mode (left) and the computational domain used in the simulations (right). The solution domain is taken as a cylindrical region between the two nozzle exit planes. The experimental configuration is rotated  $90^\circ$  in the clockwise direction to present the simulation results.

### 1.3 Objectives and challenges

The aim of this study is to demonstrate and characterize the performance of LES/PDF methodology for this experimentally studied turbulent flame that exhibits a variety of combustion regimes which (i) have practical relevance for devices such as gas turbines and combustion engines, and (ii) are known to be challenging to predict. The TCF premixed flame is extensively analyzed in experiments by conducting a parametric study on the identified critical

parameters (more details are given in Sec. 2.4). The rich experimental data enable us to assess the validity and accuracy of the models used in our code using increasing detailed modes of comparison.

## 2. Simulation details

### 2.1 Computational methodology

The turbulent premixed counterflow flame is simulated using the LES/PDF methodology. In this methodology, LES is used to represent the flow and turbulence and the PDF method is used to represent the turbulence-chemistry interactions. The filtered LES transport equations for mass, momentum and scalar (resolved specific volume) are solved on a structured grid in cylindrical coordinates by the low-Mach number, variable-density Navier-Stokes equation solver, NGA [3]. The sub-grid scale model used in the current simulations is the Lagrangian dynamic subgrid-scale model by Meneveau et al. [4].

In PDF methods [5], a large number of notional particles are distributed through out the domain. Each particle carries information on its position,  $\mathbf{X}^*(t)$ , and composition,  $\Phi^*(t)$ . The composition variable is a  $(n_s+1)$  length vector, consisting of  $n_s$  chemical species specific mole numbers,  $\mathbf{z}$  and mixture sensible enthalpy,  $h_s$ . The particle/mesh code, HPDF [6], is used to evolve the particles positions and compositions by solving the following stochastic differential equations:

$$d\mathbf{X}^*(t) = \left[ \tilde{\mathbf{U}} + \frac{\nabla[\bar{\rho}(D_T + D)]}{\bar{\rho}} \right]^* dt + [2(D_T^* + D^*)]^{1/2} d\mathbf{W}, \quad (1)$$

$$d\Phi^*(t) = -\Omega_m^*(\Phi^* - \tilde{\Phi}^*)dt + \mathbf{S}(\Phi^*)dt, \quad (2)$$

$$\Omega_m = C_m \left( \frac{D_T + D}{\Delta^2} \right), \quad (3)$$

where,

- $\mathbf{X}^*$  is the particle's position and  $\Phi^*$  is the particle's composition vector,
- $\tilde{\mathbf{U}}$  and  $\bar{\rho}$  are the resolved velocity field and mean density,
- $\mathbf{W}$  is an isotropic Wiener process,
- $D_T$  is the turbulent diffusivity,
- In this model,  $D$  is taken to be the thermal diffusivity under the unity Lewis number assumption and is obtained from the CHEMKIN's transport library,
- $\mathbf{S}(\Phi^*)$  is the source term in the composition equation,
- $\Omega_m$  is the scalar mixing frequency,  $C_m (=4.0)$  is the mixing model constant and  $\Delta$  is the LES filter width,
- Mean fields denoted with a superscript “\*” are evaluated at  $(\mathbf{X}^*(t), t)$

It is noted that the classical Interaction by Exchange with the Mean (IEM) mixing model [7] is employed in the composition equation to represent mixing and a random walk implementation is used in the particle's position equation to represent molecular transport. The chemical mechanism used in the simulations is the 16-species Augmented Reduced Mechanism (ARM1) [8]. The In-situ Adaptive Tabulation (ISAT) procedure [9] with an error tolerance of  $10^{-4}$  is used to calculate the reaction source terms in the composition equation. A two-way coupling is established between the NGA and HPDF codes by solving an additional transport equation for the resolved specific volume in NGA as described in [10]. Additionally, the resolved grid

velocities and molecular properties are transferred from the LES code to the PDF code and in return, the species mass fractions are transferred from the PDF code to the LES code.

## 2.2 Computational domain and inflow velocity boundary conditions

The computational domain in the simulations is taken as a cylindrical region between the two nozzle exit planes. This relatively small solution domain is chosen to focus on the combustion region and to make LES/PDF calculations affordable. The grid size used in the simulations is  $96 \times 96 \times 32$  with a finest z-grid spacing of  $\sim 0.1$  mm. The laminar flame length of the premixed  $\text{CH}_4/\text{O}_2/\text{N}_2$  flame with  $\phi_u = 0.85$  and  $\text{O}_2/\text{N}_2$  mole ratio of 30/70 is determined to be  $\sim 0.3$  mm. The parameters used in the base case simulation are described in Table 1.

Table 1: Simulation parameters used in the base case simulation of the turbulent premixed mode.

Simulation Parameter	Premixed Case
Opposed nozzles diameter (d)	12.7 mm
Distance b/w the nozzles ( $d_{\text{nozzle}}$ )	16 mm
Co-flow diameter	29.5 mm
Cylindrical computational domain: height, diameter	16 mm, 60 mm
Top stream	$\text{CH}_4/\text{O}_2/\text{N}_2$ ( $\phi_u = 0.85$ , $\text{O}_2/\text{N}_2$ mole ratio: 30/70) at 294 K, 1 atm. (turbulent)
Bottom stream	Hot products ( $\phi_b = 1.0$ , $\text{O}_2/\text{N}_2$ mole ratio: 26/74) at 1850 K, 1 atm. (laminar)
Bulk velocity in jets	11.2 m/s (top); 38.2 m/s (bottom)
Grid size (z, r, $\theta$ )	$96 \times 96 \times 32$
Total number of cells, particles	0.3M, 6M
Simulation time; no. of time steps	$\sim 2000$ core-hrs; $\sim 30,000$
Computational time	$\sim 26 \mu\text{s}/\text{cell}/\text{timestep}$ ; $\sim 2600$ core-hrs (NGA 30%; HPDF 70%)

The turbulence that the flame encounters is largely determined by the Turbulence Generating Plate (TGP) housed inside the top nozzle; and in contrast to jet flames, the turbulence is far from being fully-developed or locally determined. A separate nozzle simulation (including the TGP) is performed by Pettit [11] using the ‘‘PsiPhi’’ LES code to extract the time series of the three velocity components at the nozzle exit plane. These time series are used as inflow velocity boundary conditions in all the TCF simulations with appropriate modifications as follows:

$$U_i'(r, \theta, t) = \langle U_i'(r) \rangle + \alpha_i'(r)[U_i(r, \theta, \beta t) - \langle U_i(r) \rangle], \quad (4)$$

where,

- $U_i$  is the time series of the i-th component of velocity obtained from the separate nozzle simulation. The axial, radial and azimuthal velocities are denoted by  $i = 1, 2$  and  $3$  respectively.  $\langle U_i'(r) \rangle$  is the imposed mean from the experiments.
- $U_i'$  is the modified time series of velocity that has the same mean, r.m.s. and turbulent length scale at the nozzle exit plane as observed in the experiments.

## Sub Topic: Turbulent Flames

- $\alpha'_i(r)$  is a parameter that scales the fluctuations so as to match the r.m.s. velocity that is observed in the experiments.
- $\beta$  is a parameter that scales the time so as to match the turbulent length scale observed in the experiments.

This treatment successfully matches the mean and r.m.s. velocities and the turbulent length scales in the simulations to those in the experiments. This method is used to generate the velocity time series to simulate the turbulent flow in the top stream. Due to the absence of the TGP in the bottom nozzle, the bottom stream is assumed to have a laminar flow with radial profiles for the axial and radial mean velocities. The experimental data available at 2.5 mm downstream of the bottom nozzle are scaled to obtain the radial profiles. The scaling for the mean axial velocity is performed so that the volume flow rate is matched to that of the experiments and the scaling for the mean radial velocity is performed so that the mean stagnation plane is at the mid-plane.

### 2.3 Gas Mixing Layer Interface and conditional statistics approach

The procedure outlined in [2] is used for the conditional statistics analysis. In this method, the instantaneous centerline OH mass fraction profiles (obtained in the experiments using OH-LIF) are used to identify the gas mixing layer interface (GMLI) and the flame region as shown in Figure 2.

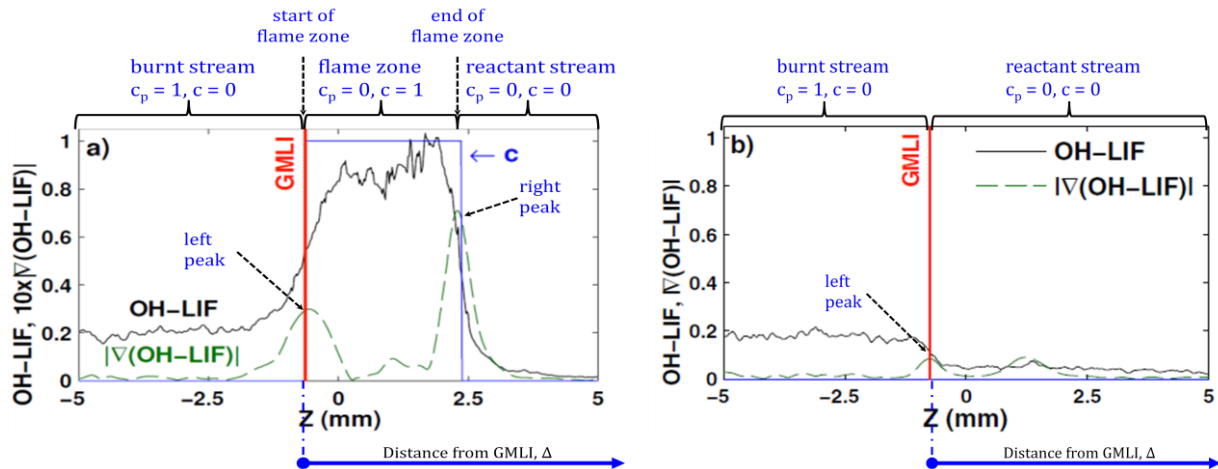


Figure 2: Detection of the GMLI and flame region using the centerline OH-LIF and  $|\nabla(\text{OH-LIF})|$  profiles. Left: intact flame front, right: local extinction. (Figure adapted from [2]).

While traversing the profiles from left to right in Figure 2, the GMLI is taken at the first peak in the  $|\nabla(\text{OH-LIF})|$  profile. The GMLI signifies the boundary that separates the two opposed streams. The flame region is identified as all pixels to the right of the GMLI that have an OH-LIF value higher than the value observed in the burnt stream. A binary-valued progress variable,  $c$ , is taken to be 1 in the flame region and 0 elsewhere. For the case of an intact flame front (Figure 2 left) we observe three distinct regions, namely burnt stream, flame zone and reactant stream. Note that the flame region is on the reactant stream side of the GMLI. For an extinguished case (Figure 2 right) we observe only the burnt stream and reactant stream regions and the OH-LIF profile drops from the observed value in the burnt stream to zero in the reactant stream without a peak. In the simulation, we use the centerline resolved OH mass fraction profiles in place of the OH-LIF signal.

## Sub Topic: Turbulent Flames

The conditional statistics analysis is performed in the reference frame attached to the GMLI. A local axial coordinate,  $\Delta$ , is defined that is parallel to the burner centerline and has an origin that is coincident with the instantaneous GMLI. The separation distance between the GMLI and flame front is denoted by  $\Delta_f$ . In the present analysis, the conditional mean progress variable  $\langle c|\Delta \rangle$  and probability density function (PDF) of local separation distance between the GMLI and flame front,  $\Delta_f$  are computed and used to study the turbulent flame behavior for different parametric conditions.

### 2.4 Parametric study of the critical parameters

The four critical parameters that are studied in the experiments for this premixed configuration are bulk strain rate  $K_{\text{bulk}}$ , turbulent Reynolds number of the top stream  $Re_t$ , equivalence ratio of the reactant stream in the top nozzle  $\phi_u$  and temperature of the hot products stream in the bottom nozzle  $T_b$ . A total of 19 cases are obtained by independently varying these critical parameters as listed in Table 2. It is to be noted that all 19 cases are important for simulations as we observe different turbulent flame behavior, both qualitatively and quantitatively, for different sets of critical parameters. In this paper, we provide the results from the computationally study of three critical parameters –  $K_{\text{bulk}}$ ,  $Re_t$  and  $\phi_u$ . The parametric study on  $T_b$  is an on-going work.

Table 2: The total number of simulation cases for the parametric study on the critical parameters of the premixed mode. The orange shading indicates the base case (case #4). The blue shading indicates the critical parameters in other cases that are different from those in the base case.

Case #	$K_{\text{bulk}}$	$Re_t$	$\phi_u$	$T_b$	$\phi_b$
1	1400	1050	Pure $N_2$	1850	1.0
2	1400	1050	0.5	1850	1.0
3	1400	1050	0.7	1850	1.0
4	1400	1050	0.85	1850	1.0
5	1400	1050	1.0	1850	1.0
6	1400	1050	1.2	1850	1.0
7	1720	1050	1.0	1850	1.0
8	2240	1050	1.0	1850	1.0
9	1400	470	0.7	1850	1.0
10	1400	470	1.0	1850	1.0
11	1400	1050	0.7	1700	1.0
12	1400	1050	1.0	1700	1.0
13	1400	1050	1.2	1700	1.0
14	1400	1050	0.7	1800	1.0
15	1400	1050	1.0	1800	1.0
16	1400	1050	1.2	1800	1.0
17	1400	1050	0.7	1950	1.0
18	1400	1050	1.0	1950	1.0
19	1400	1050	1.2	1950	1.0

## 3. Results and discussion

### 3.1 Centerline velocity statistics

Figure 3 shows the instantaneous contour plots of important quantities in the computational domain from the base case simulation. In the presented results, the experimental configuration shown in Figure 1 is rotated 90° in the clockwise direction to present these results so that the combustion products stream is on the left and the reactants stream is on the right. The turbulent premixed flame is identified by the OH mass fraction signal in the  $Y_{OH}$  contour plot.

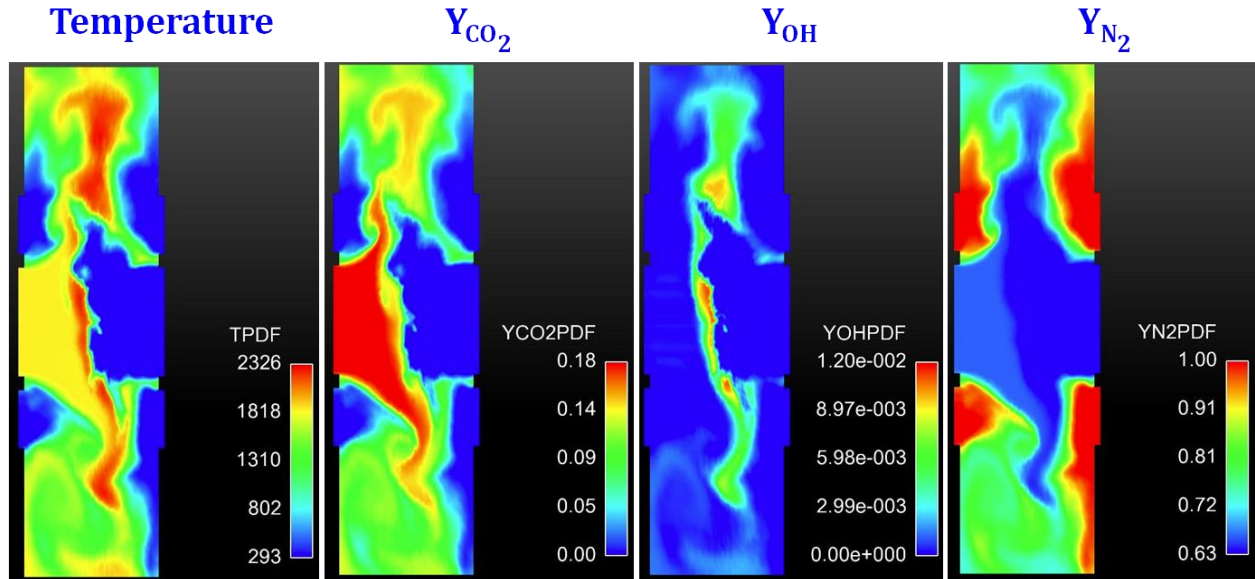


Figure 3: Instantaneous contour plots of (a) temperature (b) CO<sub>2</sub> (c) OH and (d) N<sub>2</sub> mass fractions in the solution domain from the turbulent premixed base case simulation.

Figure 4 shows the velocity statistics on the centerline connecting the two jets for the turbulent premixed base case. The mean axial velocity in the combustion products stream reaches almost twice the magnitude compared to that of the reactants stream. The comparison of the mean axial velocity with the experimental data is excellent. Also, the r.m.s. velocities match well with the experiments on the reactants stream side and subsequently go to zero on the combustion products stream side (as imposed by the boundary conditions).

### 3.2 Effect of bulk strain rate, $K_{bulk}$

The response of the turbulent premixed flame to increased bulk strain rate is studied and compared to the experiments. We find good agreement between the simulation results and the experimental data. In this study, turbulent Reynolds number, reactant equivalence ratio and product stream temperature are kept constant at values of 1050, 1.0 and 1850 K respectively. As shown in Figure 5, the probability of localized extinction at the GMLI, given by  $1 - \langle c|\Delta \rangle$  at  $\Delta=0.0$  mm, remains almost unchanged at 10% (in both the simulations and experiments) when  $K_{bulk}$  is increased from 1400 s<sup>-1</sup> to 1720 s<sup>-1</sup>. However, a further increase in the bulk strain rate to 2240 s<sup>-1</sup> significantly increases the probability of localized extinction to 40% in the experiments and to 24% in the simulations. We also note that the PDFs of the GMLI-to-flame-front distance,  $\Delta_f$ , have peaks that progressively narrow as the strain rate increases, indicating that an increased fraction of the turbulent flame fronts are in close proximity to the GMLI.

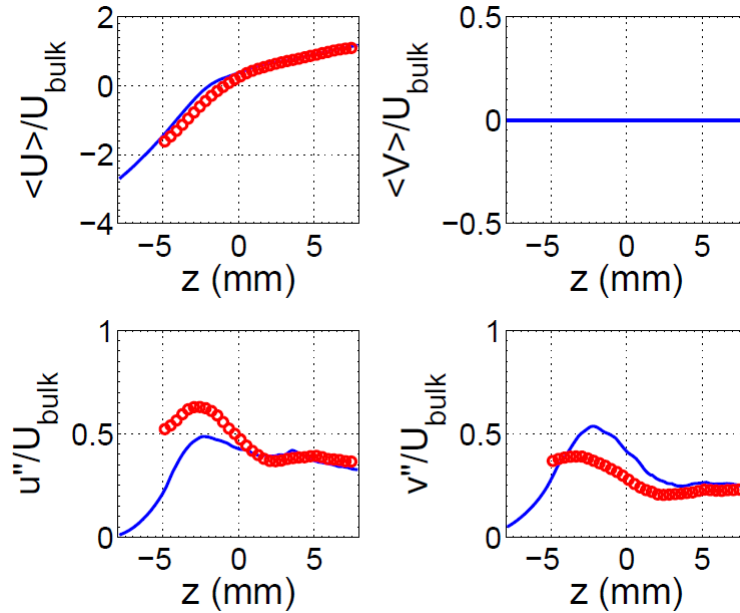


Figure 4: Velocity statistics along the centerline from the turbulent premixed base case simulation. Ordinates normalized by the bulk velocity in the top nozzle jet:  $U_{\text{bulk}} = 11.2$  m/s. Mean axial velocity: top left, mean radial velocity: top right, r.m.s. axial velocity: bottom left, r.m.s. radial velocity: bottom right. Lines: simulations, dots: experiments.

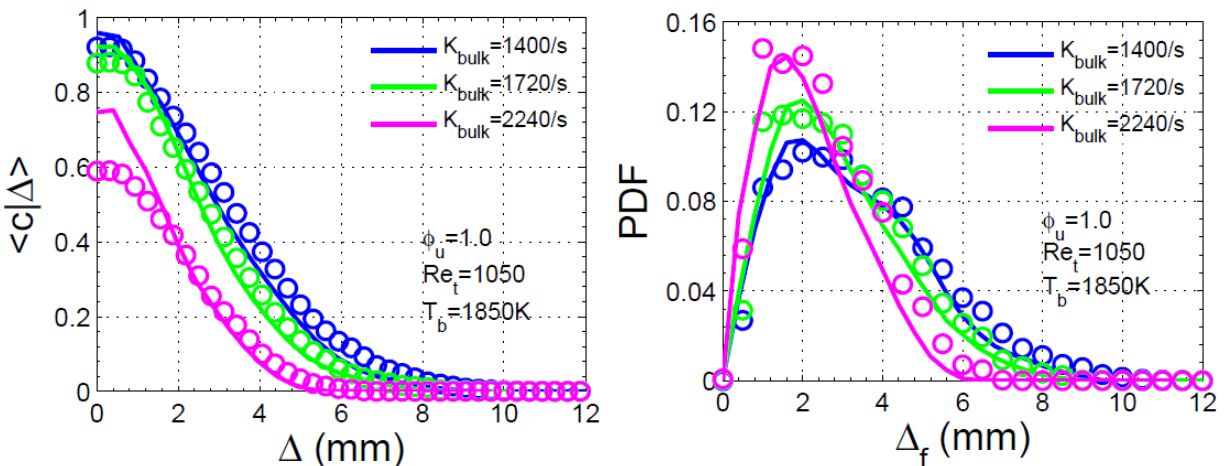


Figure 5: Effect of bulk strain rate on the stoichiometric turbulent premixed flame at turbulent Reynolds number of 1050 and product temperature of 1850 K – conditional mean progress variable as a function of distance from the GMLI,  $\Delta$  (left); PDF of local separation between the GMLI and flame front,  $\Delta_f$  (right). Lines: sim., dots: exp.

### 3.3 Effect of turbulent Reynolds number, $Re_t$

Figure 6 shows the effects of turbulent Reynolds number on the stoichiometric and lean turbulent premixed flames at  $K_{\text{bulk}} = 1400 \text{ s}^{-1}$  and  $T_b = 1850 \text{ K}$ . Clearly, there is a good agreement between the simulations and experiments. We note that the flame condition with the lowest probability of localized extinction is the stoichiometric flame with  $Re_t = 470$  with a nearly unity value of  $\langle c | \Delta \rangle$  at  $\Delta = 0.0$  mm. At the same value of  $Re_t$ , the lean flame has approximately 10% and 15% probability of localized extinction in the simulations and experiments respectively. As we



## Sub Topic: Turbulent Flames

increase  $Re_t$  from 470 to 1050, the probabilities of localized extinction for the stoichiometric and lean flames in the simulations are approximately 8% and 24% respectively. The corresponding values observed in the experiments are 10% and 40% respectively. For both values of  $Re_t$ , we also observe that the peaks of the PDFs of the separation distance,  $\Delta_f$ , observed for the lean flames are comparatively closer to the GMLI as compared to the peaks observed for the stoichiometric flames.

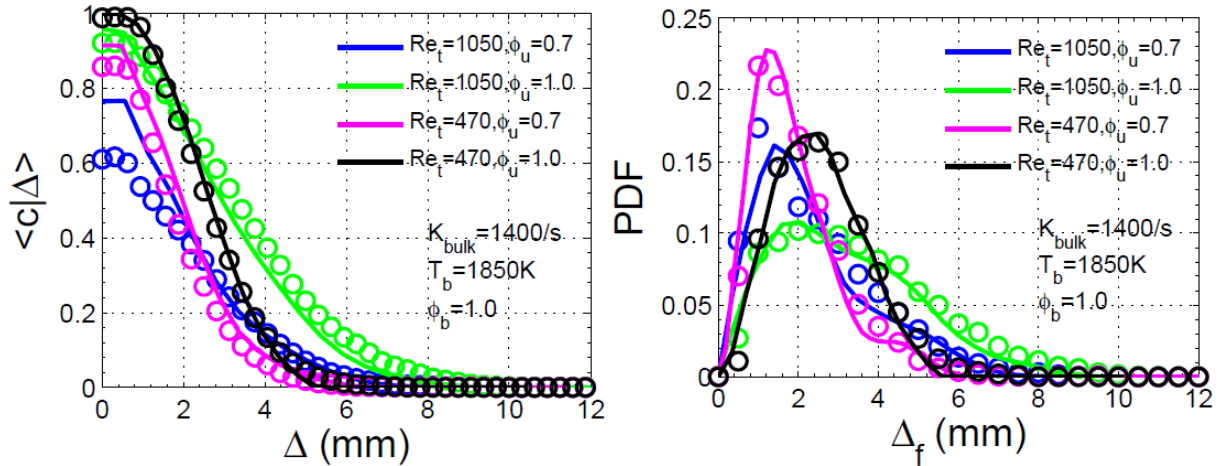


Figure 6: Effect of turbulent Reynolds number on the lean and stoichiometric turbulent premixed flame at bulk strain rate of  $1400 \text{ s}^{-1}$  and product temperature of  $1850 \text{ K}$  – conditional mean progress variable as a function of distance from the GMLI,  $\Delta$  (left); PDF of local separation between the GMLI and flame front,  $\Delta_f$  (right). Lines: sim., dots: exp.

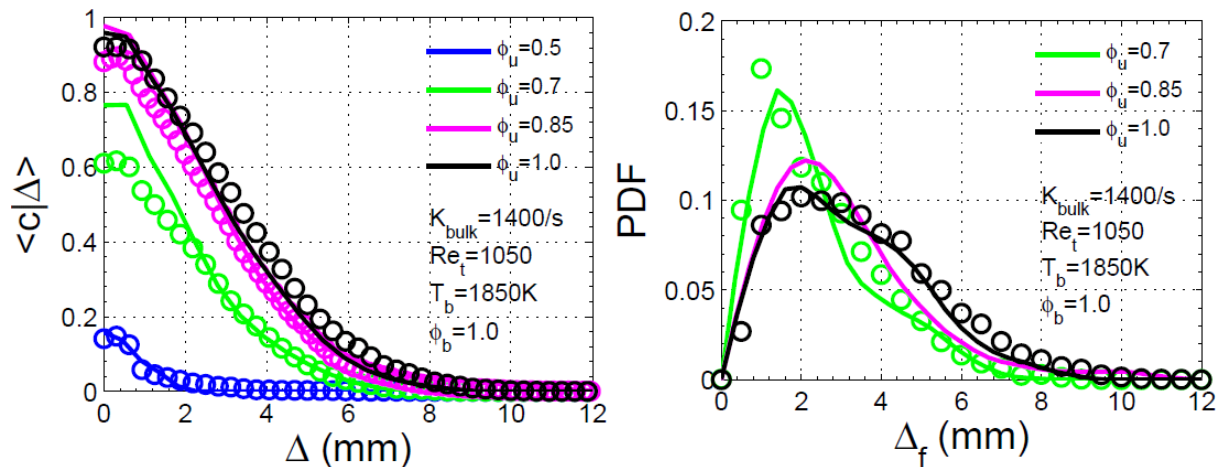


Figure 7: Effect of reactant equivalence ratio on the turbulent premixed flame at bulk strain rate of  $1400 \text{ s}^{-1}$ , turbulent Reynolds number of 1050 and product temperature of  $1850 \text{ K}$  – conditional mean progress variable as a function of distance from the GMLI,  $\Delta$  (left); PDF of local separation between the GMLI and flame front,  $\Delta_f$  (right). Lines: sim., dots: exp.

### 3.4 Effect of reactant equivalence ratio, $\phi_u$

To study the effect of reactant equivalence ratio on the turbulent premixed flame, we consider a range of values from very lean ( $\phi_u=0.5$ ) to stoichiometry ( $\phi_u=1.0$ ), while keeping the values of

$K_{\text{bulk}}$ ,  $Re_t$ ,  $T_b$  at  $1400 \text{ s}^{-1}$ , 1050 and 1850 K, respectively. Figure 7 shows that there is a good agreement between the simulation results and the experimental data. The probability of localized extinction increases as we decrease the equivalence ratio from 1.0 to 0.5. The increase is most prominent for the  $\phi_u = 0.5$  case. The probabilities of localized extinction in the simulations for  $\phi_u = 1.0, 0.85, 0.7$  and  $0.5$  are approximately 4%, 4%, 24% and 84% respectively. The corresponding experimental values are 8%, 10%, 40% and 85% respectively. It can also be observed that the peaks of PDFs move closer to the GMLI as the flame becomes leaner.

#### 4. Conclusions

In this paper, we study the effects of three critical parameters,  $K_{\text{bulk}}$ ,  $Re_t$  and  $\phi_u$ , on the turbulent premixed counterflow flame using the LES/PDF methodology. The computational domain does not include the two opposed nozzles and the specification of inflow velocity boundary conditions at the nozzle exits is challenging and non-trivial. Scaled LES data are used for the inflow velocity boundary conditions at the nozzle exit of the top nozzle which houses TGP. This treatment appears to be satisfactory. In general, good agreement is observed for the velocity statistics on the centerline. More importantly, the conditional mean progress variable,  $\langle c | \Delta \rangle$ , and the PDF of the local separation distance between the GMLI and flame front,  $\Delta_f$ , match well with the experimental data for all the parametric cases considered. Finally, it should be noted that the use of conditional statistics analysis serve to reduce the sensitivity to imperfections in the flow calculations.

#### 5. Acknowledgements

The authors thank Bruno Coriton for helping with the rich experimental data and insightful discussions. This research is funded by the U.S. Department of Energy, Office of Science, Office of Basic Energy Sciences under award number DE-FG02-90 ER14128 and earlier by the National Science Foundation under Grant CBET – 1033246. The authors thank the University of Tennessee and Oak Ridge National Laboratory Joint Institute for Computational Sciences (<http://www.jics.tennessee.edu>) and Cornell University Center for Advanced Computing (<http://www.cac.cornell.edu>) for providing the computational resources required to perform this work.

#### 6. References

- [1] G. Coppola, B. Coriton, A. Gomez, *Combust. Flame* 156 (2009), 1834-1843.
- [2] B. Coriton, J. H. Frank, A. Gomez, *Combust. Flame* 160 (2013) 2442-2456.
- [3] O. Desjardins, G. Blanquart, G. Balarac, H. Pitsch, *J. Comput. Phys.* 227 (2008), 7125-7159.
- [4] C. Meneveau, T.S. Lund, W.H. Cabot, *J. Fluid Mech.* 319 (1996), 353-385.
- [5] S. B. Pope, *Prog. Energy Combust. Sci.* 11 (1985), 119–192.
- [6] H. Wang, S.B. Pope, *Proc. Combust. Inst.* 33 (2011), 1319-1330.
- [7] J. Villermaux, J.C. Devillon, *Proc. 2nd Int. Symp. Chem. React. Eng.*, 26 (1972), 1–13.
- [8] C.J. Sung, C.K. Law, J.-Y. Chen, *Proc. Combust. Inst.* 27 (1998), 295-304.
- [9] S.B. Pope, *Combust. Theory and Model.* 1 (1997), 41-63.
- [10] Y. Yang, H. Wang, S.B. Pope, J.H. Chen, *Proc. Combust. Inst.* 34 (2013), 1241-1249.
- [11] M.W.A. Pettit, B. Coriton, A. Gomez, A.M. Kempf, *Proc. Combust. Inst.* 33 (2011), 1391-1399.